

Natural Orbitals for Wave Function Based Correlated Calculations Using a Plane Wave Basis Set

Andreas Grüneis,^{*,†} George H. Booth,[‡] Martijn Marsman,[†] James Spencer,[§] Ali Alavi,[‡] and Georg Kresse[†]

[†]Faculty of Physics and Center for Computational Materials Science, University Vienna, Sensengasse 8/12, A-1090 Vienna, Austria

[‡]Department of Chemistry, University of Cambridge, Lensfield Road, Cambridge CB2 1EW, U.K.

[§]Department of Physics and Department of Materials, Imperial College London, Exhibition Road, London SW7 2AZ, U.K.

ABSTRACT: We demonstrate that natural orbitals allow for reducing the computational cost of wave function based correlated calculations, especially for atoms and molecules in a large box, when a plane wave basis set under periodic boundary conditions is used. The employed natural orbitals are evaluated on the level of second-order Møller–Plesset perturbation theory (MP2), which requires a computational effort that scales as $O(N^5)$, where N is a measure of the system size. Moreover, we find that a simple approximation reducing the scaling to $O(N^4)$ yields orbitals that allow for a similar reduction of the number of virtual orbitals. The MP2 natural orbitals are applied to coupled-cluster singles and doubles (CCSD) as well as full configuration interaction Quantum Monte Carlo calculations of the H_2 molecule to test our implementation. Finally, the atomization energies of the LiH molecule and solid are calculated on the level of MP2 and CCSD.

INTRODUCTION

Correlated methods such as coupled-cluster theory and Møller–Plesset perturbation theory are common practice in the field of quantum chemistry. However, in their canonical formulation these methods are hard to apply to large systems and require huge computational resources. Reducing the computational cost is therefore one of the main goals in the development of correlated methods. Local correlation methods,^{1–4} pair-natural orbitals,^{5–7} explicitly correlated methods,^{8–11} optimized virtual orbitals,¹² and natural orbitals^{13–17} are among the most popular approaches to reduce the computational cost of wave function based methods. In the canonical formulation of wave function based methods, the computational cost arises in large part from the virtual orbital space. Therefore, many attempts aim at minimizing the number of virtual orbitals. Natural orbitals allow for a reduction of the virtual orbital space without compromising accuracy and are obtained easily from diagonalization of the virtual–virtual orbital block of the one-electron reduced density matrix, which can be calculated at the level of second-order Møller–Plesset perturbation theory (MP2):

$$D_{ab}^{(2)} = \sum_{cij} \frac{2\langle cb|ij\rangle\langle ij|ca\rangle - \langle cb|ji\rangle\langle ij|ca\rangle}{\Delta_{ij}^{cb}\Delta_{ij}^{ca}} \quad (1)$$

where

$$\Delta_{ij}^{cb} = \varepsilon_i + \varepsilon_j - \varepsilon_c - \varepsilon_b$$

The indices i, j and a, b, c denote occupied and unoccupied one-electron spatial orbitals, respectively, and are understood to be shorthands for both the band index and the Bloch wave vector. The ε_n correspond to one-electron Hartree–Fock eigenvalues and $\langle ij|ab\rangle$ are two-electron-four-orbital integrals. Note that the evaluation of eq 1 scales as $O(N^5)$ for atoms and molecules, where N is a measure of the system size. In ref 17, Aquilante et al.

proposed to approximate the density matrix by

$$D_{ab}^{(2)} \approx \sum_{ci} \frac{\langle cb|ii\rangle\langle ii|ca\rangle}{\Delta_{ii}^{cb}\Delta_{ii}^{ca}} \quad (2)$$

This allows for calculating an *approximate MP2 density matrix* with a computational effort that scales as $O(N^4)$ only.

Eigenvectors and eigenvalues of the density matrix are called (approximate) MP2 natural orbitals and occupation numbers, respectively. The occupation numbers lie between 0 and 1, and those extreme values imply that the corresponding natural orbital occurs in none or all configurations (excited Slater determinants), respectively.¹³ We stress that only virtual orbitals are mixed by $D_{ab}^{(2)}$.

If Gaussian-type orbitals (GTOs) are used, natural orbitals allow for a reduction of the virtual orbital space by about one-half without significantly compromising accuracy.^{14–16} But Gaussian-type orbitals are already spatially confined to the regions around the atoms, and much larger reductions are possible if a spatially delocalized, unbiased basis set is used to capture correlation effects.

Plane waves (PWs) fall into this category. They have undeniable advantages; in particular, their precision and completeness can be arbitrarily improved by increasing a single parameter, the PW energy cutoff. Plane waves are very efficient for conventional density functional theory or Hartree–Fock calculations if iterative algorithms are used to determine the occupied orbitals only.¹⁹ Similar iterative algorithms are not yet available for many-electron wave function based methods. The advantages of plane waves then turn into a severe handicap: the number of virtual orbitals becomes intractable very quickly. Fortunately, most of the variational degrees of freedom are irrelevant for the description of the many-electron wave function, in particular, for

Received: April 16, 2011

Published: July 05, 2011

atoms or molecules in a large box, where several thousand plane waves are required to achieve total energy convergence. A large part of this variational space is unnecessary, because it describes regions in the vacuum far away from the nucleus, where the true many-electron wave function vanishes. In the following, it is shown that one can lift this problem by means of natural orbitals that are calculated at the level of MP2 or in an even more approximate fashion. This allows for the efficient calculation of the electronic correlation energy using highly sophisticated many-electron methods, such as coupled-cluster or full configuration interaction quantum Monte Carlo (FCIQMC) methods, which have previously been limited to more compact basis sets such as GTOs.

■ COMPUTATIONAL DETAILS

The density matrix in eq 1 is calculated using the Vienna ab initio simulation package (VASP) in the framework of the projector-augmented wave (PAW) method.^{18–20} In the PAW method, the one-electron orbitals ψ are derived from the pseudo-orbitals $\tilde{\psi}$ by means of a linear transformation

$$|\psi\rangle = |\tilde{\psi}\rangle + \sum_i (|\phi_i\rangle - |\tilde{\phi}_i\rangle) \langle \tilde{p}_i | \tilde{\psi} \rangle \quad (3)$$

The pseudo-orbitals $\tilde{\psi}$ are the variational quantities of the PAW method and are expanded in reciprocal space using plane waves. The index i is a shorthand for the atomic site \mathbf{R}_i , the angular momentum quantum numbers l_i and m_i , and an additional index ε_i denoting the linearization energy.¹⁹ The all-electron partial waves ϕ_i are the solution to the radial Schrödinger equation for the non-spin-polarized reference atom at specific energies ε_i and specific angular momentum l_i . The pseudopartial waves, $\tilde{\phi}_i$, are equivalent to the all-electron partial waves outside a core radius r_c and match continuously onto ϕ_i inside the core radius. The partial waves ϕ_i and $\tilde{\phi}_i$ are represented on radial logarithmic grids. The projector functions \tilde{p}_i are constructed in such a way that they are dual to the pseudopartial waves, i.e.,

$$\langle \tilde{p}_i | \tilde{\phi}_j \rangle = \delta_{ij} \quad (4)$$

As a result of the transformation, any local operator (e.g., density) can be expressed as a sum of three terms:

$$A = \langle \tilde{\psi} | A | \tilde{\psi} \rangle - \sum_{ij} [\langle \tilde{\phi}_i | A | \tilde{\phi}_j \rangle \langle \tilde{\psi} | \tilde{p}_i \rangle \langle \tilde{p}_j | \tilde{\psi} \rangle + \langle \phi_i | A | \phi_j \rangle \langle \tilde{\psi} | \tilde{p}_i \rangle \langle \tilde{p}_j | \tilde{\psi} \rangle] \quad (5)$$

The first term is a pseudized contribution evaluated on a plane wave grid, whereas the second and third terms are corrections to account for the shape difference between the pseudized orbitals $|\tilde{\psi}\rangle$ and the exact all-electron orbitals $|\psi\rangle$. They are calculated separately for each atomic site using atom centered grids (i.e., only one-center contributions are required). The terms $\langle \tilde{\phi}_i | A | \tilde{\phi}_j \rangle$ and $\langle \phi_i | A | \phi_j \rangle$ are the expectation values of the operator A in an LCAO (linear combination of atomic orbitals) basis, where the first and second basis set describes the pseudized orbitals and the exact all-electron orbitals, respectively. The efficiency of the method relates to the fact that only one-center corrections are required, since all long-range contributions are (exactly) described by the first term. Similar expressions are obtained for the two-electron integrals (see ref 21 for details). Since a more detailed introduction to the PAW method is beyond the scope of

this work, we refer the reader to the seminal paper of Blöchl¹⁸ and the work of Kresse and Joubert.²⁰

The evaluation of the two-electron–four-orbital integrals $\langle ij | ab \rangle$ in the PAW method is thoroughly discussed in ref 21 and requires two plane wave basis sets: (i) the basis set for the one-electron orbitals $\psi_i(\mathbf{r})$, $\psi_j(\mathbf{r})$, $\psi_a(\mathbf{r})$, and $\psi_b(\mathbf{r})$ as well as (ii) the auxiliary basis set used in the construction of the overlap density between two orbitals $\psi_i^*(\mathbf{r})\psi_a(\mathbf{r})$. These basis sets are determined by all PWs $e^{i\mathbf{G}\cdot\mathbf{r}}$ with wavevectors \mathbf{G} satisfying the equations

$$(\hbar^2/2m_e)|\mathbf{G}|^2 < E_{\text{cut}}$$

and

$$(\hbar^2/2m_e)|\mathbf{G}|^2 < E_\chi$$

respectively.

As such, the energy cutoff E_{cut} determines the basis set for the one-electron orbitals, whereas the cutoff E_χ defines a basis set for densities (products of two orbitals) that is analogous to auxiliary basis sets used in density fitting.²² For the evaluation of $D_{ab}^{(2)}$ we set E_χ close to E_{cut} because we find a fast convergence of the natural orbitals with respect to E_χ . The correlation energy in the complete basis set limit, however, is extrapolated by systematically increasing E_χ at fixed E_{cut} . The exact extrapolation procedure is outlined in ref 21.

In this work, we used a newly developed coupled-cluster singles and doubles (CCSD) module in VASP and the FCIQMC code from ref 23 that was interfaced with VASP. Coupled-cluster theory^{24–26} is a very successful method for describing electronic correlation in atoms and molecules.²⁷ In particular, CCSD(T) is known for achieving chemical accuracy (1 kcal/mol) in the prediction of atomization and reaction energies for a wide class of molecules.²⁷ We apply the CCSD method to three-dimensional fully periodic systems. Our CCSD implementation employs the working equations published in refs 28–30 and reduces the memory requirements by evaluating all two-electron–four-orbital integrals on-the-fly. The FCIQMC method by Booth et al.²³ constitutes a recently developed and very efficient way to calculate the exact full CI ground state energy of a many-electron system by solving the imaginary-time Schrödinger equation stochastically. We will not repeat the expressions of the CCSD and FCIQMC methods, but we refer the reader to refs 28–30 and 23, 31–33 for details, respectively.

Natural orbitals with an occupation number close to zero are expected to contribute only little to the correlation energy.¹³ Therefore, we introduce a threshold, ξ , that defines a subspace of the natural orbitals by truncating them according to their occupation number. Only natural orbitals with an occupation number larger than ξ are included in this subspace.

Unlike HF orbitals, natural orbitals do not diagonalize the HF Hamiltonian. Therefore, noncanonical formulations of the employed correlated methods would be required. We use a standard recanonicalization to avoid the necessity for noncanonical implementations by carrying out the following procedure subsequent to the underlying Hartree–Fock (HF) calculation: (i) calculate the natural orbitals (NOs), (ii) order the natural orbitals according to their occupation numbers (eigenvalues of $D_{ab}^{(2)}$), (iii) recalculate the HF Hamiltonian in the basis of NOs, and (iv) diagonalize the HF Hamiltonian in a truncated subspace defined by those natural orbitals with occupation numbers above a threshold ξ . These “canonicalized” orbitals diagonalize

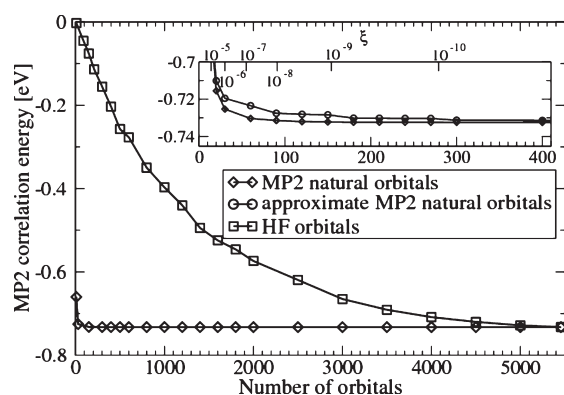


Figure 1. Convergence of the MP2 correlation energy of the Li atom in a $6 \times 6 \times 6 \text{ \AA}^3$ box with respect to the number of natural and HF orbitals per spin-channel. The inset shows the convergence on a different scale. The top axis in the inset shows the occupation number threshold, ξ , of the MP2 natural orbitals for the spin-up channel.

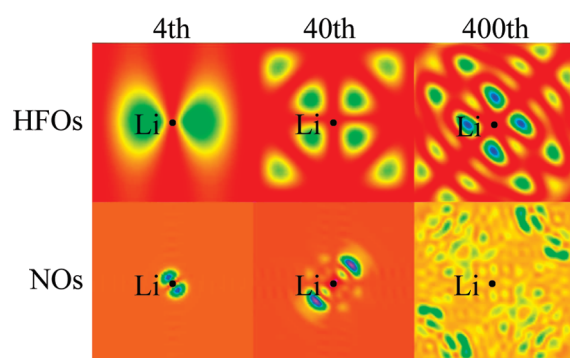


Figure 2. Charge densities of the Hartree–Fock orbitals (HFOs) in the top row and natural orbitals (NOs) in the bottom row of a Li atom in a $6 \times 6 \times 6 \text{ \AA}^3$ box. The fourth, 40th, and 400th orbitals have been plotted.

the Hartree–Fock Hamiltonian in the truncated subspace and can be used in a subsequent canonical wave function based correlated calculation. We stress that the correlation energy is not changed by the diagonalization in the subspace of NOs since the occupied orbital space is always unchanged.

In the calculations of the atomization energies of the molecular systems (H_2 and LiH), we minimize the interaction between the periodic images by extrapolating the contribution from the correlation energy according to a $1/V^2$ behavior to $V \rightarrow \infty$, where V corresponds to the unit cell volume. This procedure has already been outlined in ref 21. To obtain the atomization energies of solids, we use large cubic boxes with 9 \AA length in the calculations of the isolated atoms.

NATURAL MP2 ORBITALS

Natural MP2 Orbitals. As a first example, we study the convergence of the MP2 correlation energy of a spin polarized Li atom in a $6 \times 6 \times 6 \text{ \AA}^3$ box. The correlation energy was not extrapolated to the complete basis set limit; instead, a fixed kinetic energy cutoff of $E_{\chi} = 400 \text{ eV}$ was used. The kinetic energy cutoff for the one-electron orbitals was set to $E_{\text{cut}} = 500 \text{ eV}$. Figure 1 shows the MP2 correlation energy of the Li atom with respect to the number of orbitals per spin channel. For the given cutoff and box size, 5450 orbitals span the complete space of

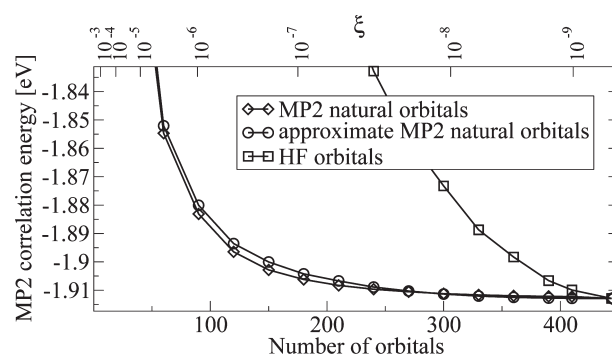


Figure 3. Convergence of the MP2 correlation energy of the LiH solid using a $4 \times 4 \times 4$ k -point mesh with respect to the number of natural and HF orbitals per k -point. The top axis shows the occupation number threshold, ξ , of the MP2 natural orbitals at the Γ -point.

one-electron Hartree–Fock orbitals (HFOs). The convergence of the correlation energy with respect to the number of HFOs is extremely slow. Even 4000 HFOs yield an MP2 correlation energy that deviates by more than 10 meV from the correlation energy obtained using the full space (733 meV). In contrast, 30 natural orbitals (NOs) already suffice to obtain an agreement that is within 10 meV of the converged value. The top axis of the inset in Figure 1 shows the corresponding occupation number threshold, ξ , of the MP2 natural orbitals, indicating that 30 natural orbitals correspond to an occupation number threshold of 10^{-6} . The occupation numbers quickly decay to zero, which illustrates the insignificance of the neglected natural orbitals and the “redundancy” present in the PW basis set in the description of many-electron properties. Approximate MP2 natural orbitals (eigenvectors of the approximate density matrix given by eq 2) reduce the convergence rate only slightly (see inset of Figure 1). In fact, both types of natural orbitals allow for reducing the number of virtuals compared to Hartree–Fock by at least an order of magnitude.

Figure 2 shows the charge densities of the fourth, 40th, and 400th natural and Hartree–Fock orbital of a Li atom in a $6 \times 6 \times 6 \text{ \AA}^3$ box. Hartree–Fock orbitals and natural orbitals are ordered by their increasing one-electron HF eigenvalues and decreasing occupation numbers, respectively. The HF orbitals become essentially plane waves at higher energies and greater band indices, since the kinetic energy operator dominates at sufficiently high energies. The natural orbitals with large occupation numbers maximize the overlap with the occupied orbitals, whereas the natural orbitals with small occupation numbers exhibit only very little density at the Li atom, as can be clearly seen for the 400th NO.

Figure 3 shows the convergence of the MP2 correlation energy of the face-centered-cubic LiH crystal with a unit cell volume of 17.03 \AA^3 . The first Brillouin zone was sampled using a $4 \times 4 \times 4$ k -point mesh and the same cutoffs as for the Li atom were employed ($E_{\chi} = 400 \text{ eV}$, $E_{\text{cut}} = 500 \text{ eV}$). In the case of solids, the reduction of the virtual orbital space using natural orbitals is less significant than for a single atom in a box. This is not unexpected, because in contrast to an atom in a box, the electrons of the solid are delocalized over the entire unit cell and almost all degrees of freedom supplied by the plane wave basis set are required to describe the many-electron wave function. Nevertheless, it is possible to remove about half of the full HF virtual orbital space without introducing an error larger than 10 meV. Note that a

Table 1. Atomization Energies of the LiH Molecule in the HF, MP2, and CCSD Approximation Using Natural and HF Orbitals^a

| | this work | ref 21 | GAMESS |
|----------------------------|-----------|--------|----------------|
| basis set type | PWs | PWs | aug-cc-pV[TQ]Z |
| orbitals | NOs | HFOs | HFOs |
| ΔE^{HF} | 1.084 | 1.084 | 1.085 |
| ΔE_c^{MP2} | 0.823 | 0.822 | 0.818 |
| ΔE_c^{CCSD} | 1.039 | | 1.034 |

^a Plane-waves (PWs) as well as aug-cc-pVXZ (X=T,Q) basis sets were used in the calculations. The results obtained using aug-cc-pVXZ basis sets were extrapolated to $X \rightarrow \infty$ assuming a functional form of $1/X^3$ for the correlation energy. All energies in eV.

reduction in the number of virtual orbitals by a factor of 2 reduces the computational cost in MP2 calculations by a factor of 4. The approximate and exact MP2 natural orbitals show a very similar convergence rate. The top axis in Figure 3 shows the corresponding occupation number thresholds, ξ , for the MP2 natural orbitals. An error smaller than 10 meV in the correlation energy can be achieved by including all NOs with $\xi = 10^{-7}$.

Natural MP2 orbitals for CCSD and FCIQMC. As a first test of our implementation we calculate the dissociation energy of the H₂ molecule with a bond length of 0.75 Å using 80 natural orbitals. Both the CCSD as well as the FCIQMC method were applied. Since for a two-electron system CCSD accounts for all possible excitations from the HF determinant into excited Slater determinants, it should yield exact results, as does the full CI quantum Monte Carlo method. Indeed, our FCIQMC and CCSD results agree exactly. We obtain a HF and FCIQMC contribution to the dissociation energy of 3.619 and 1.112 eV, respectively. Likewise, the resulting dissociation energy of 4.731 eV agrees with the experimental value of 4.73 eV.³⁴

As a second test of our implementation we have calculated the dissociation energy of the LiH molecule at the level of MP2 as well as CCSD using NOs. The bond length was set to 2.042 Å. This bond length corresponds to the nearest neighbor distance in the LiH solid at the unit cell volume of 17.03 Å³. Table 1 summarizes the HF, MP2, as well as CCSD contributions to the atomization energies of the LiH molecule. The column on the right lists the results that have been obtained using the GTO GAMESS code.^{35–37} The middle column summarizes the HF and MP2 results that were calculated using a PW basis set and Hartree–Fock orbitals in ref 21. The column on the left summarizes the HF, MP2, as well as CCSD contributions obtained using PWs and NOs. The PW and GTO results agree to within a few millielectronvolts. The discrepancy between the PW MP2 results obtained using NOs and HFOs is 1 meV and originates from the truncation of the virtual orbitals in the natural orbital basis. A total of 200 and 58 NOs were used in the calculations of the molecule and atom, respectively corresponding to an occupancy threshold ξ of approximately 10^{-7} . For comparison, we note that the aug-cc-pVQZ basis set consists of 126 and 80 orbitals in the LiH molecule and Li atom, respectively. The agreement of the CCSD result calculated using PWs with the one obtained using the GTO basis is very good as well, with the PW result being approximately 5 meV lower in energy than the GTO result. This is excellent considering that VASP employs the PAW method and is not a conventional GTO all-electron code.

Table 2. Contributions of the MP2 Correlation Energy to the Atomization Energy of the LiH Crystal Calculated According to eq 6^a

| m_{NOs} | m_3 | m_4 | ΔE_c^{MP2} |
|------------------|-------|-------|---------------------------|
| 192 | 16 | 16 | 1.192 |
| 256 | 16 | 16 | 1.195 |
| 192 | 32 | 16 | 1.203 |
| 192 | 48 | 16 | 1.189 |
| 192 | 54 | 16 | 1.189 |
| 192 | 64 | 16 | 1.205 |
| 192 | 54 | 32 | 1.185 |
| 192 | 54 | 48 | 1.187 |

^a All energies in eV.

Table 3. HF, MP2, and CCSD Contributions to the Atomization Energy of the LiH Crystal Using Different Orbitals Compared to Quantum Chemical Calculations Deducing the Atomization Energy from LiH Clusters Using an Incremental Approach (ref 40)^a

| | this work | ref 21 | ref 40 |
|----------------------------|-----------|--------|--------|
| orbitals | NOs | HFOs | HFOs |
| ΔE^{HF} | 3.583 | 3.583 | 3.589 |
| ΔE_c^{MP2} | 1.187 | 1.188 | 1.182 |
| ΔE_c^{CCSD} | 1.326 | | 1.329 |

^a The MP2 contribution to the atomization energy of the LiH crystal from ref 21 corresponds to a calculation using a $4 \times 4 \times 4$ k -point mesh. All energies in eV.

At this point we want to stress that the calculations of the LiH molecule summarized above and in ref 21 were not carried out at the experimental equilibrium bond length (1.596 Å).³⁸ MP2 and CCSD calculations using NOs at the experimental bond length of the LiH molecule yield an atomization energy of 2.33 and 2.52 eV, respectively. The experimental dissociation energy corrected for the zero-point energy amounts to 2.52 eV.³⁸ As expected, CCSD corrects for the underestimation present in MP2 and deviates from experiment by less than 10 meV.

As a last application, we calculate the atomization energy of the LiH solid on the level of MP2 as well as CCSD. Even with natural orbitals, it would be impossible to perform a CCSD calculation of the LiH crystal with a k -point mesh denser than $2 \times 2 \times 2$, because of the large number of virtual orbitals and the unfavorable scaling of the computational effort of CCSD with respect to the system size. Therefore, we use an approach similar to the progressive downsampling technique of Ohnishi et al. in ref 39, relying on the observation that the long-range behavior of the correlation energy depends mostly on the low-lying excitations. We approximate the correlation energy, \hat{E}_c , of a solid for $(K \times K \times K)$ k -points and m_{full} orbitals per k -point with

$$\hat{E}_c(K \times K \times K, m_{\text{full}}) = E_c(2 \times 2 \times 2, m_{\text{full}}) + \sum_{k=3}^K C_k \quad (6)$$

$E_c(2 \times 2 \times 2, m_{\text{full}})$ is the calculated correlation energy using a $(2 \times 2 \times 2)$ k -point mesh and a converged basis set. C_k are correction terms that account for the difference between

($2 \times 2 \times 2$) and denser k -point grids. Those corrections are calculated according to

$$C_k = E_c(k \times k \times k, m_k) - E_c((k-1) \times (k-1) \times (k-1), m_k)$$

In practice, we find a fast convergence of C_k with respect to m_k . This allows the denser k -point meshes to be calculated with fewer bands per k -point since only the energy difference between the k -point meshes is required.

Evidently eq 6 becomes exact for $m_k \rightarrow m_{\text{full}}$, but typically m_k is chosen significantly smaller than m_{full} and decreases with an increasing number of k -points, k . Moreover, we note that $E_c(2 \times 2 \times 2, m_{\text{full}})$ is calculated using m_{NOs} natural orbitals at each k -point.

Table 2 summarizes the convergence of the MP2 atomization energy with respect to m_{NOs} and m_i for all k . We find that the convergence with respect to m_k is fairly noisy. From the noise, we estimate an error bar of approximately 10 meV for the correlation energy given by eq 6. To attain this accuracy, it suffices to use $m_{\text{NOs}} = 192$, $m_3 = 54$, and $n_4 = 32$ to reproduce straightforward MP2 calculations.

These values are then employed in a CCSD calculation. Table 3 summarizes the resulting HF, MP2, and CCSD contributions to the atomization energy of the LiH crystal. The results are compared to previous calculations obtained using Gaussian type orbitals and standard quantum chemical methods combined with the incremental approach, which extrapolates the correlation energy from LiH clusters of increasing size.⁴⁰ For MP2, the agreement between refs 21 and 40 was already discussed in ref 21. The first important observation is that the extrapolation procedure eq 6 works reliably for the MP2 contribution to the atomization energy of the LiH crystal. Our MP2 results deviate by less than 10 meV from those of ref 21. In passing, we note that periodic local MP2 results for the cohesive energy of the LiH crystal published in ref 41 also agree to within 10 meV with our values. Moreover, our CCSD results are in very good agreement with ref 40, which gives us confidence in the correct implementation of the CCSD code for periodic boundary conditions.

The resulting MP2 and CCSD atomization energies deviate from the experimental atomization energy corrected for zero point vibrations (4.974 eV⁴²) by 204 and 65 meV, respectively. As such, CCSD clearly outperforms MP2 and is likely to capture more of the correct physics in the case of the LiH solid.

CONCLUSIONS AND OUTLOOK

In summary, we have shown that MP2 natural orbitals allow for a tremendous reduction of the virtual orbital space, compared to HF orbitals for calculations of atoms or molecules in a box using a PW basis set. For the atoms and molecules considered here, the basis set is typically reduced by a factor of 10–100 compared to untruncated canonical HF plane wave orbitals. The reduction allows for calculations of atoms and small molecules using highly accurate quantum-chemical methods such as CCSD and even FCIQMC in a PW basis set. In the case of solids, the virtual orbital space can be reduced approximately by half without compromising the accuracy significantly. Note that in CCSD calculations, a reduction of the virtual orbital space by half corresponds to a speed-up of an order of magnitude. Although the computational cost of evaluating natural orbitals scales as $O(N^5)$, we can approximate the MP2 NOs by a simpler expression that scales only as $O(N^4)$. The approximated NOs perform

only slightly worse than the exact MP2 NOs. This even allows us to reduce the computational cost of MP2 calculations for large systems. But natural orbitals will not only help in expanding the applicability of our MP2 or CCSD implementation. Many other correlated methods that are implemented in a PW basis will benefit as well. It is straightforward to apply the presented procedures to other methods such as the random-phase approximation plus second-order screened exchange⁴³ or GW-BSE.⁴⁴ We hope to use this formalism to greatly expand the scope of wave function based periodic methods in a PW basis set. Moreover, future prospects shall include the development of an FCIQMC algorithm that will enable us to treat solid-state systems using complex orbitals and arbitrary k -point meshes.

AUTHOR INFORMATION

Corresponding Author

*E-mail: ag618@cam.ac.uk.

ACKNOWLEDGMENT

This work was supported by the Austrian Fonds zur Förderung der wissenschaftlichen Forschung (FWF) within the SFB ViCom (F41) and the START grant. Most of the calculations have been performed in the Vienna Scientific Cluster (VSC).

REFERENCES

- (1) Pulay, P.; Saebo, S. *Theor. Chim. Acta* **1986**, 69, 357.
- (2) Saebo, S.; Pulay, P. *Annu. Rev. Phys. Chem.* **1993**, 44, 213.
- (3) Schütz, M.; Hetzer, G.; Werner, H.-J. *J. Chem. Phys.* **1999**, 111, 5691.
- (4) Subotnik, J.; Head-Gordon, M. *J. Chem. Phys.* **2005**, 123, 064108.
- (5) Meyer, W. *Int. J. Quantum Chem.* **1971**, S5, 341.
- (6) Meyer, W. *J. Chem. Phys.* **1973**, 58, 1017.
- (7) Nesse, F.; Wennmohs, F.; Hansen, A. *J. Chem. Phys.* **2009**, 130, 114108.
- (8) Hättig, C.; Tew, D. P.; Köhn, A. *J. Chem. Phys.* **2010**, 132, 231102.
- (9) Klopper, W.; Samson, C. C. M. *J. Chem. Phys.* **2002**, 116, 6397.
- (10) Werner, H. J.; Adler, T. B.; Manby, F. R. *J. Chem. Phys.* **2007**, 126, 164102.
- (11) Shiozaki, T.; Hirata, S. *J. Chem. Phys.* **2010**, 132, 151101.
- (12) Neogrady, P.; Pitonák, M.; Urban, M. *Mol. Phys.* **2005**, 103, 2141.
- (13) Löwdin, P.-O. *Phys. Rev.* **1995**, 97, 1474.
- (14) Taube, A. G.; Bartlett, R. J. *Collect. Czech. Chem. Commun.* **2005**, 70, 837.
- (15) Taube, A. G.; Bartlett, R. J. *J. Chem. Phys.* **2008**, 128, 164101.
- (16) Rolik, Z.; Kállay, M. *J. Chem. Phys.* **2011**, 132, 124111.
- (17) Aquilante, F.; Todorova, T. K.; Gagliardi, L.; Pedersen, T. B.; Roos, B. O. *J. Chem. Phys.* **2009**, 131, 034113.
- (18) Blöchl, P. E. *Phys. Rev. B* **1994**, 50, 17953.
- (19) Kresse, G.; Furthmüller, J. *Phys. Rev. B* **1996**, 54, 11169.
- (20) Kresse, G.; Joubert, D. *Phys. Rev. B* **1999**, 59, 1758.
- (21) Marsman, M.; Grüneis, A.; Paier, J.; Kresse, G. *J. Chem. Phys.* **2009**, 130, 184103.
- (22) Maschio, L.; Usvyat, D.; Manby, F. R.; Casassa, S.; Pisani, C.; Schütz, M. *Phys. Rev. B* **2007**, 76, 075101.
- (23) Booth, G. H.; Thom, A. J. W.; Alavi, A. *J. Chem. Phys.* **2009**, 131, 054106.
- (24) Coester, F. *Nucl. Phys.* **1958**, 1, 421.
- (25) Coester, F.; Kümmel, H. *Nucl. Phys.* **1960**, 17, 477.
- (26) Čížek, J. *J. Phys. Chem.* **1966**, 45, 4256.
- (27) Bartlett, R. J.; Musial, M. *Rev. Mod. Phys.* **2007**, 79, 291.

- (28) Hirata, S.; Grabowski, I.; Tobita, M.; Bartlett, R. J. *Chem. Phys. Lett.* **2001**, *345*, 475.
- (29) Hirata, S.; Podeszwa, R.; Tobita, M.; Bartlett, R. J. *J. Chem. Phys.* **2004**, *120*, 2581.
- (30) Hirata, S. *J. Phys. Chem. A* **2003**, *107*, 9887.
- (31) Cleland, D.; Booth, G. H.; Alavi, A. *J. Chem. Phys.* **2010**, *132*, 041103.
- (32) Booth, G. H.; Alavi, A. *J. Chem. Phys.* **2010**, *132*, 174104.
- (33) Cleland, D. M.; Booth, G. H.; Alavi, A. *J. Chem. Phys.* **2011**, *134*, 024112.
- (34) Huber, K.P.; Herzberg, G. *Molecular Spectra and Molecular Structure. Constants of Diatomic Molecules*; Van Nostrand Reinhold: New York, 1979; Vol. IV, 716 pp.
- (35) <http://www.msg.chem.iastate.edu/GAMESS/GAMESS.html>, 4.7.2011
- (36) Schmidt, M. W.; Baldridge, K. K.; Boatz, J. A.; Elbert, S. T.; Gordon, M. S.; Jensen, J. H.; Koseki, S.; Matsunaga, N.; Nguyen, K. A.; Su, S. J.; Windus, T. L.; Dupuis, M.; Montgomery, J. A. *J. Comput. Chem.* **1993**, *14*, 1347.
- (37) Gordon, M. S.; Schmidt, M. W. In *Theory and Applications of Computational Chemistry: The First Forty Years*; Elsevier: New York, 2005; Chapter 41, pp 1167–1189.
- (38) Trail, J. R.; Needs, R. J. *J. Chem. Phys.* **2008**, *128*, 204103 and references therein.
- (39) Ohnishi, Y.-y.; Hirata, S. *J. Chem. Phys.* **2010**, *133*, 034106.
- (40) Nolan, S. J.; Gillan, M. J.; Alfé, D.; Allan, N. L.; Manby, F. R. *Phys. Rev. B* **2009**, *80*, 165109.
- (41) Usvyat, D.; Civalleri, B.; Maschio, L.; Dovesi, R.; Pisani, C.; Schütz, M. *J. Chem. Phys.* **2011**, *134*, 214105.
- (42) Schimka, L.; Harl, J.; Kresse, G. *J. Chem. Phys.* **2011**, *134*, 024116.
- (43) Grüneis, A.; Marsman, M.; Harl, J.; Schimka, L.; Kresse, G. *J. Chem. Phys.* **2009**, *131*, 154115.
- (44) Albrecht, S.; Reining, L.; Del Sole, R.; Onida, G. *Phys. Rev. Lett.* **1998**, *80*, 4510.